Available online at www.sciencedirect.com
SCIENCE DIRECT®
Journal of Nuclear Materials 350 (2006) 19–39
journal of nuclear materials
www.elsevier.com/locate/jnucmat

On the thermal conductivity of UO_2 nuclear fuel at a high burn-up of around 100 MWd/kgHM

C.T. Walker [a,*], D. Staicu [a], M. Sheindlin [a], D. Papaioannou [a], W. Goll [b], F. Sontheimer [b]

[a] European Commission, Joint Research Centre, Institute for Transuranium Elements, P.O. Box 2340, D-76125 Karlsruhe, Germany
[b] AREVA-Framatome ANP GmbH, P.O. Box 3223, D-91050 Erlangen, Germany

Received 14 October 2005; accepted 16 November 2005

Abstract

A study of the thermal conductivity of a commercial PWR fuel with an average pellet burn-up of 102 MWd/kgHM is described. The thermal conductivity data reported were derived from the thermal diffusivity measured by the laser flash method. The factors determining the fuel thermal conductivity at high burn-up were elucidated by investigating the recovery that occurred during thermal annealing. It was found that the thermal conductivity in the outer region of the fuel was much higher than it would have been if the high burn-up structure were not present. The increase in thermal conductivity is a consequence of the removal of fission products and radiation defects from the fuel lattice during recrystallisation of the fuel grains (an integral part of the formation process of the high burn-up structure). The gas porosity in the high burn-up structure lowers the increase in thermal conductivity caused by recrystallisation.

1. Introduction

Knowledge of the radial temperature distribution in UO_2 fuel during irradiation is essential to the successful prediction of fuel performance at high burn-up. This is because the fuel operating temperature affects, amongst other things, fission product migration, fission gas release, grain growth and swelling. Moreover, the thermal stresses that are associated with steep radial temperature gradients can cause the fuel to plastically deform at the centre or crack at the outside during a reactor power transient. Of the various factors affecting the fuel operating temperature one of the most important is the fuel thermal conductivity. This is not constant during irradiation but decreases with burn-up due to a combination of the build-up of fission products, the formation of gas porosity and radiation damage in the UO_2 lattice.

With rise in the burn-up at which nuclear fuel assemblies are discharged from the reactor, the acquisition of data on degradation of thermal conductivity with burn-up has become increasingly important. Particularly since it was observed that when the pellet burn-up exceeds 40–45 MWd/kgHM, the UO_2 grains in the outer region of the

* Corresponding author. Tel.: +49 7247 951 477; fax: +49 7247 951 590.
E-mail address: clive.walker@itu.fzk.de (C.T. Walker).

0022-3115/$ - see front matter © 2005 Elsevier B.V. All rights reserved.
doi:10.1016/j.jnucmat.2005.11.007

fuel pellet begin to recrystallise [1]. The transformed microstructure, which is referred to as the high burn-up structure, consists of small, recrystallised grains of average size 0.15 μm and a high concentration of gas filled pores (up to 15 vol.% at the pellet rim [2]) of typical diameter 1–2 μm [2,3]. Because of its high porosity, theory indicates that the high burn-up structure has a lower thermal conductivity than untransformed fuel and that its presence would cause the temperature in the interior of the fuel pellet to rise, increasing fission gas release and fuel swelling.

The OECD Halden Reactor Project (HRP) was one of the first to respond to the need for information on the degradation of the thermal conductivity of UO_2 fuel with rise in burn-up. Between 1989 and 1995, in the frame of their fuels and materials testing programme, the HRP carried out a systematic study of the increase in fuel operating temperature with burn-up up to 75 MWd/kgUO_2 (86 MWd/kgU) [4,5]. In this study, centre-line temperatures were measured in-pile in fuel rods instrumented with expansion thermometers. The rods used in the study contained highly enriched fuel (e.g., 13% ^{235}U), had a small fuel-cladding gap (100 μm diametrical) and were filled with helium. Moreover, during irradiation the rod power was regulated so that the centre temperature of the fuel did not exceed the fission gas release threshold. It was found [5] that, owing to the degradation in thermal conductivity, the centre temperature of the fuel increased by about 250 °C on irradiation to 75 MWd/kgUO_2 at a linear power of 25 kW m^{-1}. The degradation in the thermal conductivity, λ, derived from the in-pile fuel centre temperature measurements carried out by the Halden Project is given by

$$\lambda = \frac{1}{0.1148 + 0.0035B + 2.475 \times 10^{-4}(1 - 0.003B)T + 0.0132e^{0.00188T}}, \quad (1)$$

where T is the local fuel temperature in °C, B is the local burn-up in MWd/kgUO_2 and λ is the thermal conductivity in W m^{-1} K^{-1} for a fuel of 95% TD. This correlation indicates that between 250 and 1000 °C the thermal conductivity of UO_2 decreases by 6–7% per 10 MWd/kgHM. It is pointed out that temperature measurements made during the first hours of irradiation failed to detect the steep fall in thermal conductivity reported by Daniel and Cohen [6] and Lokken and Courtright [7] and attributed by them to radiation damage. As a result, Wiesenack [5] concluded that radiation damage had only a small effect on the thermal conductivity of UO_2 at the temperatures encountered in-pile, and that it is insufficient to explain the recovery of thermal diffusivity observed in out-of-pile laser flash measurements.

Lucuta et al. [8] have studied the effect of burn-up on thermal conductivity, using UO_2 doped with fission product elements to simulate burn-ups of 3 and 8 at.% (roughly 29 and 76 MWd/kgHM, respectively) termed SIMFUEL [9]. The thermal conductivity was derived from the thermal diffusivity that was measured by the laser flash method [10] and a modulated electron-beam method [11]. They also observed that the thermal diffusivity of the UO_2 decreased with increase in the simulated burn-up. The percentage decrease, however, was less than that reported by Wiesenack for irradiated fuel (2.5–5.5% per 10 MWd/kgHM in the temperature range 250–1000 °C). Moreover, the thermal conductivity values measured by Lucuta et al. [8] were markedly higher (e.g., 2.4 W m^{-1} K^{-1} at 1000 °C at a burn-up of 76 MWd/kgHM compared with 1.8 W m^{-1} K^{-1}). The difference is mainly explained by the fact that the major fission product elements Cs and Xe are not present in SIMFUEL. The absence of Xe is a particular drawback, because in irradiated fuel it has a large influence on the thermal conductivity since it forms gas bubbles and pores, which decrease the fuel density. It is also to be noted that at 76 MWd/kgHM the porous high burn-up structure is wide spread in the outer region of UO_2 fuel, but it is not present in SIMFUEL because there is no radiation damage. Using the same material, Lucuta et al. [12] investigated the effect of stoichiometry on thermal conductivity. They found that at temperatures below 600 °C, the thermal conductivity of hypostoichiometric SIMFUEL decreased with increase in the simulated burn-up, but was unaffected at higher temperatures. They also report that at a given burn-up the thermal conductivity of SIMFUEL decreased with increase in the degree of hypostoichiometry (i.e., increase in the oxygen potential of the material).

More recently, Ronchi et al. [13] using the laser flash method measured the thermal diffusivity of UO_2 disc fuel from the High Burn-up Rim Project (HBRP) (see e.g., Ref. [14]). The disc fuel, which had burn-ups in the range 32–96 MWd/kgU, differed from power reactor fuel in three main ways. First, it was highly enriched to enable the target

burn-up to be reached rapidly. Second, the radial burn-up profile was relatively flat and a radial temperature gradient was not present during irradiation. Third, and perhaps most importantly, cladding constraint was absent during irradiation. Ronchi et al. [13] found, as expected, that the thermal diffusivity of the irradiated discs decreased with rise in burn-up. The largest decrease was observed in a fuel disc that had been irradiated to a burn-up of 92 MWd/kgU at a low temperature of 450 °C. Most significantly, Ronchi et al. observed that the thermal diffusivity of the irradiated fuel discs recovered during annealing and that the degree of recovery increased with the annealing temperature. An important conclusion from this study is that the high burn-up structure does not have a detrimental effect on the fuel thermal conductivity, as was assumed by many, but has a positive effect, since it limits the decrease of thermal diffusivity with burn-up. Yagnik reports [15] that the NFIR programme had performed a very similar fuel disc irradiation shortly before the inception of HBRP and that thermal diffusivity measurements by laser flash were also carried out on the irradiated discs. The findings were very similar to those reported by Ronchi et al. [13]. Moreover, there is broad agreement that the fission product inventory is principally responsible for the degradation of the thermal conductivity of UO_2 with rise in burn-up and that the recovery caused by thermal annealing can be explained by the repair of radiation damage and the removal of fission products from solid solution. It is to be noted that Kinoshita et al. [16] compared the thermal diffusivity results for the irradiated discs from the NFIR Programme and HBRP and showed that they are consistent. On plotting the measured thermal diffusivity as a function of the disc burn-up Kinoshita et al. observed that the thermal diffusivity decreased only slightly at a burn-up of 60 MWd/kgHM, which is the local burn-up threshold for the formation of the high burn-up structure [17,18]. They deduced from this that formation of the high burn-up structure is not accompanied by a significant degradation in fuel thermal conductivity. The good agreement between the thermal diffusivity data generated by the NFIR programme and HBRP clearly reflects the broad similarities that exist in the fuel disc and rod design characteristics and between the histories of the two irradiations that were performed in the Halden boiling water reactor (HBWR).

To the knowledge of the authors only Carrol et al. [19], Nakamura et al. [20] and Ohira and Itagaki [21] have used the laser flash method to measure the thermal diffusivity of irradiated power reactor fuel pellets. Their results confirm those obtained on disc fuel in the sense that the UO_2 thermal diffusivity was seen to be lower after irradiation and it was found that thermal annealing resulted in recovery. Carrol et al. [19] carried out laser flash measurements on fuel with a burn-up of approximately 40 MWd/kgU from the Halden IFA 558 irradiation. Nakamura et al. [20] measured the thermal diffusivity of UO_2 fuel with a burn-up 63 MWd/kgU, which had also been irradiated in the HBWR. In contrast, Ohira and Itagaki [21] investigated the thermal conductivity of UO_2 fuel irradiated to 61 MWd/kgU in a commercial BWR. They also comment that the observed degradation in thermal conductivity was larger than that exhibited by SIMFUEL [8].

The present paper describes a study of the thermal conductivity of a commercial PWR fuel with an average section burn-up of 102 MWd/kgHM. The thermal conductivity data reported were derived from thermal diffusivity measurements made using the laser flash method. The factors determining the fuel thermal conductivity at high burn-up were elucidated by investigating the recovery that occurred during thermal annealing. The irradiated fuel has been characterised in detail using a wide range of post-irradiation examination techniques. For example, the radial distributions of fission products Nd and Xe, and Pu have been measured by electron probe microanalysis (EPMA). The Nd radial concentration profile is used as an indicator of the radial burn-up distribution in the pellet. Moreover, the radial porosity distribution in the fuel has been measured using optical microscopy in combination with quantitative image analysis. Further, the extent of formation of the high burn-up structure in the fuel has been established using optical and scanning electron microscopy. In addition, inductively coupled plasma mass spectrometry (ICP-MS) was used to determine the concentration of the actinide isotopes in the fuel. From the ICP-MS results the specific activity of the fuel was calculated and the extent of self-irradiation during storage of the spent fuel prior to the laser flash measurements being performed was obtained. Thus, the paper provides a comprehensive account of the thermal conductivity of LWR fuel at ultra-high burn-up.

2. Fuel characteristics and irradiation history

The fuel pellet and rod design characteristics are given in Table 1. The rods were of standard PWR design for Siemens built reactors with plenum space above and below the fuel stack. The fuel cladding was a highly corrosion resistant zirconium alloy.

The rods were irradiated in Siemens built 15×15 fuel assemblies in a commercial PWR reactor. The irradiation, which spanned nine reactors cycles and lasted 2913 effective full power days (EFPD), ended in June 1997. At the end of the fourth irradiation cycle, when the original fuel assembly reached its nominal discharge burn-up in the region of 60 MWd/kgHM, rod 12C3, from which the fuel samples for thermal diffusivity measurement were taken, was transferred to a carrier assembly containing partially burnt fuel. The rod was subsequently introduced into a new carrier assembly at the start of each new reactor cycle.

Table 2 shows the power history and burn-up evolution of fuel rod 12C3. It is seen that during the first four reactor cycles the average power rating fell from 34 to 20 kW m^{-1}. During irradiation in the carrier assemblies the power rating decreased gradually from 18 kW m^{-1} in the fifth cycle to 14 kW m^{-1} in the ninth and final cycle. At the end-of-life the rod average burn-up was 97.8 MWd/kgHM.

Table 1
Fuel pellet and rod design characteristics

Pellet diameter (mm)	9.3
Initial enrichment (wt% ^{235}U)	3.5
Fuel density (% TD)	95
2D grain size[a] (μm)	9–12
O/M	2.005
Diametrical gap (μm)	160–190
He fill gas pressure (bar)	22.5
Cladding material	Zr-based alloy

[a] Linear intercept.

Table 2
Power history and burn-up evolution in the high burn-up fuel rod

Reactor cycle	Maximum average linear power (kW m^{-1})	Cumulative average burn-up (MWd/kgHM)
1	34	19
2	29	37
3	23	48
4	20	59
5	18	67
6	17	72
7	16	82
8	14	90
9	14	98

3. Fuel samples on which diffusivity measurements were made

The thermal diffusivity measurements were performed on two 1 mm thick discs cut from the upper end of the fuel stack of rod 12C3 within 15 mm of the location of the samples taken for optical microscopy, EPMA and SEM [23]. The average burn-up of the discs, therefore, was assumed to be similar to that of these samples, which was determined by chemical burn-up analysis to be 102 MWd/kgHM.

An important variable influencing the thermal diffusivity of nuclear fuel during irradiation is the fuel temperature since the phonon mean free path should vary as $1/T$. Rod 12C3 was irradiated at low temperatures. The radial temperature profile in the upper end of the fuel stack of rod 12C3 during the eighth irradiation cycle is shown in Fig. 1. It is seen that fuel centre temperature was around 950 °C and that in the outer region of the fuel where the high burn-up structure was present the temperature varied from about 370 to 720 °C. Apparently, the radial temperature profile changed little during the last four reactor cycles. Moreover, indications are that it would not have been significantly affected by a 20% reduction in power rating during the last two weeks of the irradiation.

The radial profile shown in Fig. 1 was calculated with the advanced version of the Framatome ANP fuel rod analysis and design code CARO-E [24]. This code makes allowance for the degradation of the thermal conductivity of UO_2 fuel with increase in burn-up; both due to the build-up of fission products in the UO_2 lattice and the presence of small gas pores in the high burn-up structure. Knowledge of the fuel temperature during the final stages of irradiation is a basic requirement for the correct interpretation of the thermal diffusivity results since it determines the concentration of irradiation defects in the spent fuel and thereby affects the measured values.

4. Post-irradiation examination results relevant to this study

4.1. Radial burn-up distribution

The radial burn-up distribution was determined from the local concentration of fission product Nd

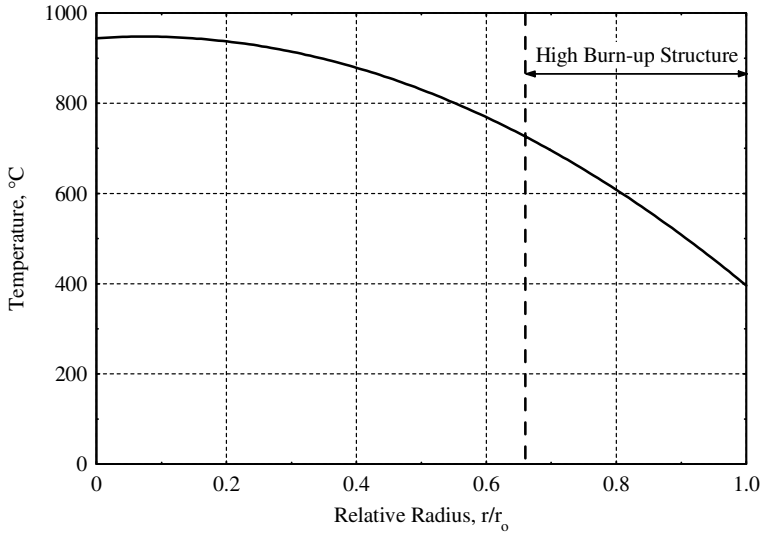

Fig. 1. Radial temperature distribution in the high burn-up fuel samples during the last irradiation cycle as calculated with the CARO-E fuel rod analysis and design code (Ref. [24]).

measured by EPMA using the procedure described in Ref. [23]. The resulting burn-up profile is shown in Fig. 2. It can be seen from the figure that in the body of the fuel the local burn-up is slightly less than the pellet average burn-up of 102 MWd/kgHM, whereas at the fuel surface it is around 2.5 times higher. The steep increase in burn-up at the fuel surface is due to the fission of Pu created by neutron capture [25].

4.2. Radial distribution of plutonium

The radial distribution of Pu was measured by EPMA using the procedure described in Ref. [25]. The creation of Pu during the irradiation of UO_2 nuclear fuel is the result of capture of epithermal neutrons in the resonances of ^{238}U. The measured radial concentration profile for Pu is shown in Fig. 3. Like the radial profile for Nd that for Pu is

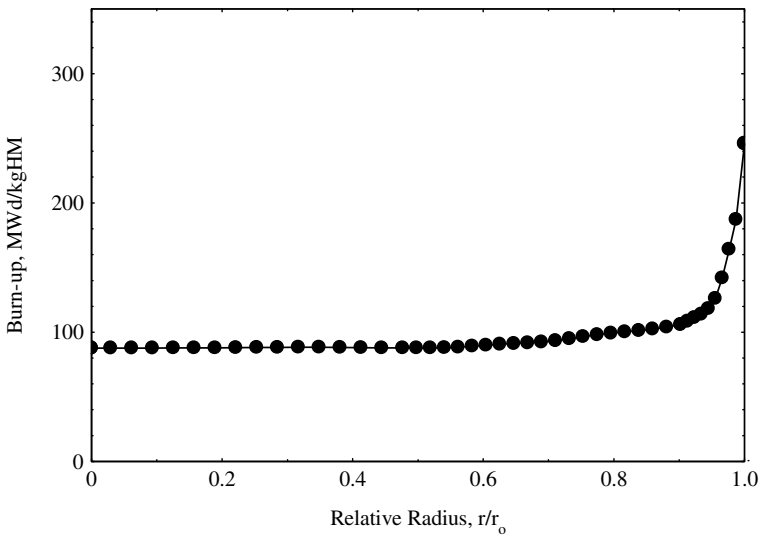

Fig. 2. Radial burn-up distribution in the high burn-up fuel samples as determined from the local concentration of fission product neodymium measured by EPMA.

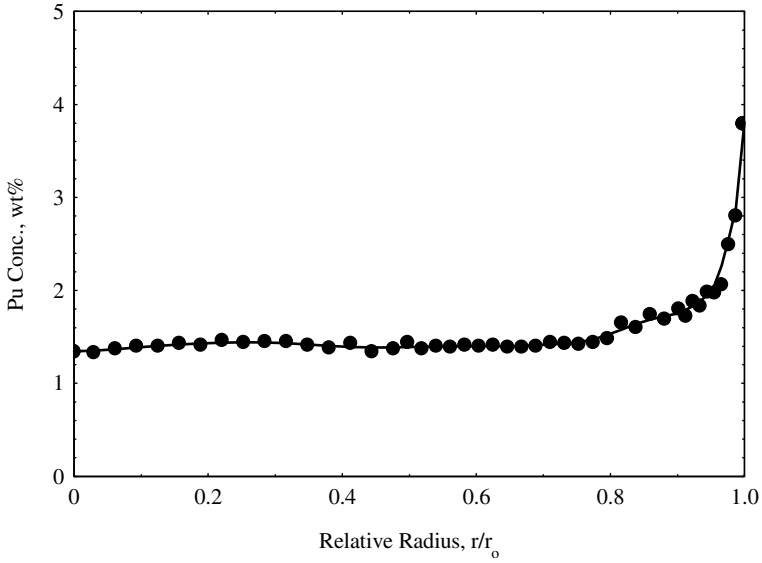

Fig. 3. The radial distribution of Pu in the high burn-up fuel samples as measured by EPMA.

flat in the interior of the fuel and increases steeply at the fuel rim. The profile indicates that at the end of the irradiation the integral average concentration of Pu in the fuel was 1.62 wt%.

4.3. Radial distribution of retained xenon

The Radial distribution of retained Xe was measured by EPMA using the procedure reported in Ref. [23]. The measured radial concentration profile is shown in Fig. 4. It can be seen from the figure that over the whole pellet cross-section only a small fraction (0.15–0.3 wt%) of the created Xe concentration (pellet average 1.4 wt%) was retained in the fuel grains.

4.4. Radial porosity distribution

The local porosity was determined using quantitative image analysis carried out on optical micro-

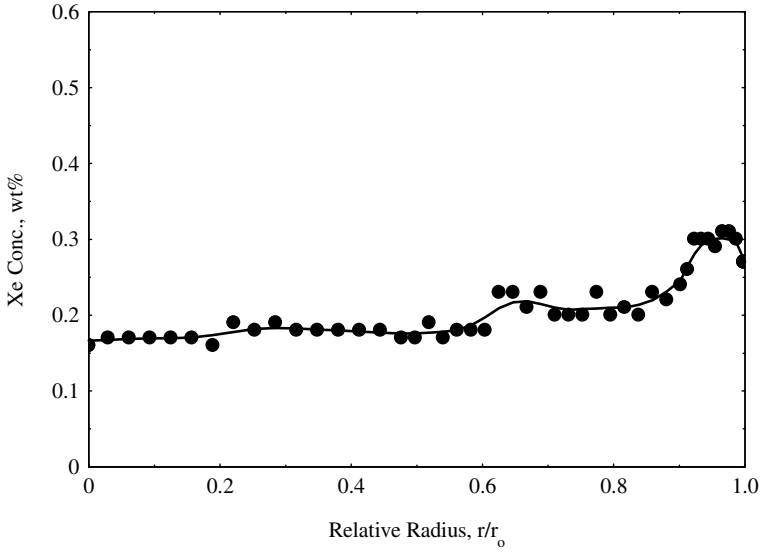

Fig. 4. Radial distribution of fission product Xe in the high burn-up fuel samples as measured by EPMA.

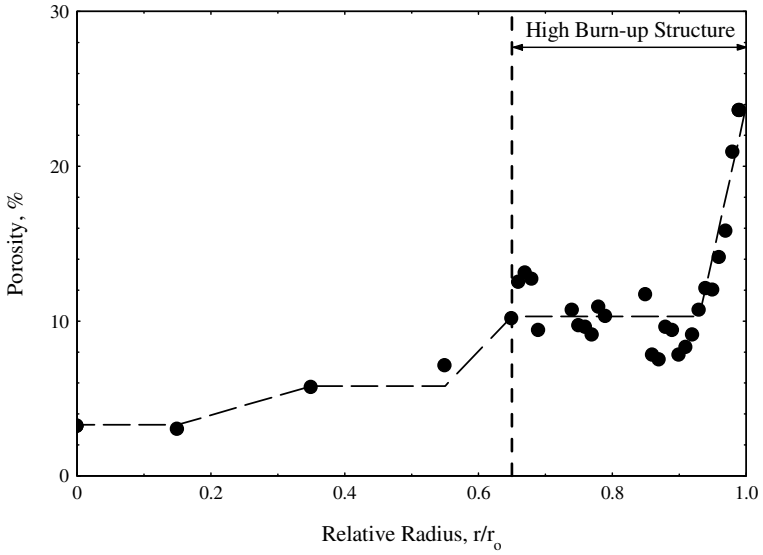

Fig. 5. Radial distribution of porosity in the high burn-up fuel samples as measured by optical microscopy. The broken line drawn through the data point serves to guide the eye.

graphs produced at a magnification of 500×. The measured radial porosity profile is shown in Fig. 5. In the central region of the fuel the porosity, which was mainly a consequence of open gas escape channels at grain edges, ranged from 3% at the pellet centre to 6% at $r/r_0 = 0.55$. The high burn-up structure extended from the pellet rim to about $r/r_0 = 0.65$ and resulted in an increase in porosity to around 10% at the latter radial position. The porosity of the high burn-up structure remained at around this level until about $r/r_0 = 0.93$ when it exhibited a sharp rise, reaching 24% at the pellet surface. This was the direct result of an extraordinary increase in the size of the gas pores of the high burn-up structure in the rim region of the pellet [23].

4.5. Specific alpha activity of the fuel

The specific alpha activity of the fuel was determined from the concentrations of the actinide isotopes measured by ICP-MS in January 2004 [26]. The measured concentrations of the actinide nuclides and their specific alpha activity are given in Table 3. From the data in the table the specific activity of the fuel was calculated to be 4.5 GBq g^{-1}.

4.6. Microstructure of the fuel

The microstructure of the fuel was examined by optical microscopy and SEM. Both techniques revealed that the high burn-up structure (see Fig. 6), penetrated from the fuel surface to about $r/r_0 = 0.65$. In the intermediate region between $r/r_0 = 0.48$ and 0.65, grain sub-division had occurred but without the formation of the gas pores, which are characteristic of the high burn-up structure. The small grain size is attributed [23] to recrystallisation that probably began at the earliest during the sixth irradiation cycle and continued during the whole period of extended irradiation. In the central region of the fuel, between the pellet centre and $r/r_0 = 0.48$, grain growth and thermal fission gas

Table 3
ICP-MS results for the concentrations of the actinide isotopes in the fuel and the specific alpha activity of the isotope

Nuclide	Concentration (wt%)	Specific alpha activity (Bq g^{-1})
^{234}U	0.010	2.30×10^8
^{235}U	0.014	8.00×10^4
^{236}U	0.369	2.39×10^6
^{237}Np	0.086	2.60×10^7
^{238}U	77.768	1.24×10^4
^{239}Pu	0.502	2.30×10^9
^{240}Pu	0.348	8.39×10^9
^{241}Pu[a]	0.113	9.36×10^7
^{241}Am	0.075	1.27×10^{11}
^{242}Pu	0.265	1.46×10^8
^{243}Am	0.104	7.38×10^9
^{244}Cm	0.116	2.99×10^{12}
^{245}Cm	0.013	6.35×10^9
^{246}Cm	0.009	1.14×10^{10}

[a] Decays mainly by β^- emission with a half-life of 14.4 yrs, but a small branching probability to α-decay exists.

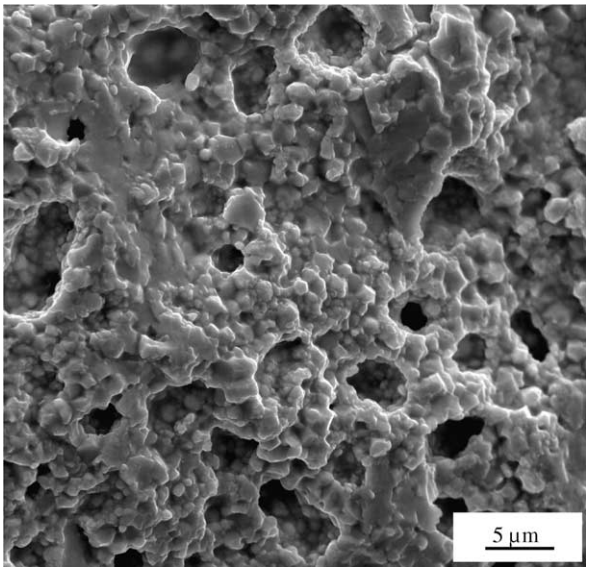

Fig. 6. Appearance of the high burn-up structure at $r/r_0 = 0.99$ in the high burn-up fuel samples. The local burn-up is about 210 MWd/kgHM.

release had occurred. Accordingly, the microstructure exhibited equi-axed grains up to 20 μm in size and large pores at grain boundary triple points.

4.7. Radial variation of the O/U ratio of the fuel

The local O/U of the fuel was determined from the lattice parameter measured by micro-X-ray diffraction [27] after correction for the concentrations of fission products and Pu dissolved in the fuel lattice and correction for radiation damage [26]. The O/U ratios derived from lattice parameter measurements are plotted as a function of radial position in Fig. 7. It can be seen that between the pellet centre and $r/r_0 = 0.89$ the O/U ratio varied between 1.989 and 1.995. Thus, at all the radial positions where the thermal diffusivity was measure the UO_2 matrix was slightly hypostoichiometric.

5. Elucidation of the factors determining the thermal conductivity of irradiated UO_2 nuclear fuel at high burn-up

It is generally accepted that the thermal conductivity, λ, of UO_2 is dominated by phonon heat transport that is well described at temperatures below about 1500 °C by the relation [22]:

$$\lambda = \frac{1}{A + BT}, \tag{2}$$

where the coefficient A is a measure of the concentration of phonon scattering centres in the lattice that mainly consist of point defects and fission product atoms in solid solution, and the coefficient B represents the intrinsic thermal resistivity of the UO_2 lattice resulting from scattering between phonons. The numerical values of the coefficients A and B are determined from regression lines fitted to scatterplots of $\frac{1}{\lambda}$ versus T. Ronchi et al. [13] used

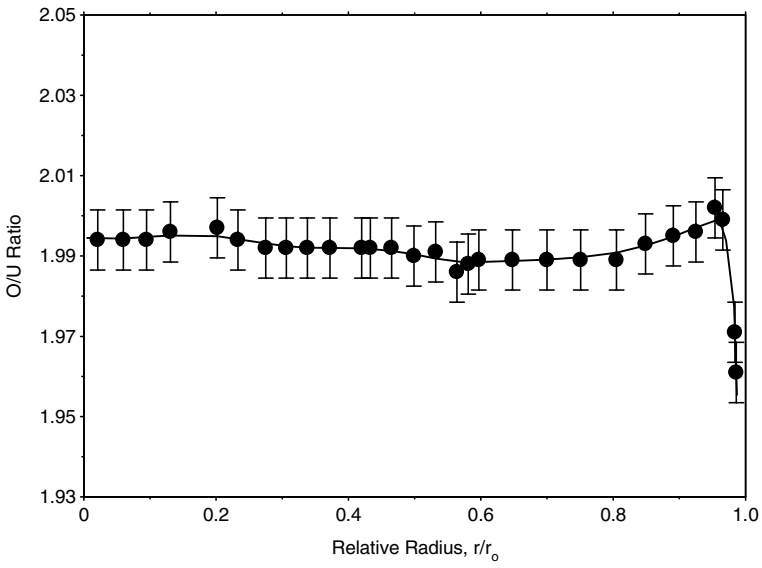

Fig. 7. Radial variation in the O/U ratio of the high burn-up fuel samples derived from lattice parameter measurements (Ref. [27]).

sequential thermal annealing to reveal the factors determining the thermal conductivity of UO_2 nuclear fuel during irradiation. They found that the recovery in thermal conductivity caused by annealing was accompanied by a decrease in the value of coefficient A and an increase in the value of coefficient B. Moreover, they showed that both coefficients A and B exhibited two recovery steps, one in the temperature range 850–1000 K; the other between 1200 and 1300 K. The first recovery step they attributed to the annihilation of point defects created in-pile and the second to the coalescence of fission product atoms in solid solution to form voids and solid precipitates. At annealing temperatures below the irradiation temperature of the fuel disc, Ronchi et al. [13] observed a small decrease in the coefficient A of around 0.02 mK W^{-1} which was explained by the healing of self-irradiation defects produced during storage of the spent fuel before the thermal diffusivity measurements were made.

6. Experimental

6.1. Measurement of thermal diffusivity

A shielded laser flash device, LAF-1, was used to measure thermal diffusivity. The device was designed and built at the Institute for Transuranium Elements specifically for measurements on irradiated nuclear fuel. The fuel sample is heated to the measurement temperature in a HF induction furnace. A heat pulse is then produced on the lower surface of the sample using a Nd-YAG pulse laser. The temperature increase at the upper surface of the sample caused by the laser heat pulse is measured using a high-speed pyrometer (0.05 °C sensitivity) with a response time of around 100 μs.

Sheindlin et al. [28] show a diagram and give a description of the device in its current form. The specimen chamber is contained inside a lead-shielded glove box. The specimen stage, which is a sapphire disc on which the sample is placed, is located inside the induction furnace, which is a graphite cylinder heated by a copper coil. The highest temperature obtainable with the furnace is 1500 °C. Located above the sample stage is a water-cooled objective lens that is connected by an optical fibre to the detectors of the pyrometer. The diameter of the area on the sample over which the temperature is measured can be varied between 0.6 and 1.0 mm depending on the diameter of the optical fibre, which serves as a field stop aperture. The fibre is built into an optical mirror that allows observation of the complete cross-section of the sample with a portable telescope and facilitates the exact determination of the position on the sample of the thermal diffusivity measurement.

The laser is situated outside the shielded glove box and the laser beam is transferred to the sample by way of focusing system that is located outside the sample chamber and which is connected to the laser head by a second optical fibre. The focal spot at the sample surface can be varied between 2 and 5 mm without the introduction of a significant radial power gradient.

The thermal diffusivity of the high burn-up fuel from rod 12C3 was measured on irregular shaped fuel fragments several millimetres in size, broken from the two discs samples. On one fragment the thermal diffusivity at approximately the pellet mid-radial position ($r/r_0 = 0.55$) was measured; on the other the variation in the thermal diffusivity with radial position was measured. The thermal diffusivity at $r/r_0 = 0.55$ was measured in the irradiated condition starting at a temperature of 284 °C, and after annealing at six temperatures in the range 359–837 °C. The variation in the thermal diffusivity with radial position was measured in the irradiated condition starting at 217 °C and after annealing at 317 and 452 °C. The samples were heated in a low pressure atmosphere of 10^{-3} mbar N_2. The time required to reach thermal equilibrium decreased with the measurement temperature from 1.5 h at 250 °C to 10 min at 830 °C. Experience has shown that holding the sample at the measurement temperature for longer periods does not lead to any measurable supplementary recovery of the thermal diffusivity. When the temperature was stable, a laser pulse of energy density roughly 1000 Jm^{-2} and of duration 10 ms was fired at the fuel sample. The relatively long pulse length reduced the level of thermal shock experienced by the fuel sample. The diameter of the laser beam was slightly larger than the sample and the radial power distribution within the beam was homogeneous. Thus, the temperature pulse generated can be described by a plane wave travelling through the material in the axial direction. This greatly simplifies calculation of heat transfer within the sample. The temperature recorded was the average value in an area measuring 1 mm in diameter. The thermogram, $T = T(t)$, recorded with the high-speed pyrometer consisted of several thousand data points and was analysed using a mathematical expression for the propagation of the energy pulse

in the material that takes into account the experimental time profile of the laser energy deposition. The thermal diffusivity was then calculated together with the heat loss coefficients using a numerical fitting procedure. This was followed by a self-consistency check that involved reconstruction of the experimental thermogram [28]. Cracks and holes in the fuel where the thermal diffusivity is measured cause temperature perturbations in the thermograms. Measurements producing thermograms exhibiting temperature perturbations were discarded. For irradiated nuclear fuel the accuracy of the thermal diffusivity results is of the order of ±5%.

The radial variation of the thermal diffusivity was determined from local measurements made at several radial positions between $r/r_0 = 0.08$ and 0.81. For local measurements of the thermal diffusivity the optical fibre and mirror are moved by step motors over the sample surface; the sample itself is not displaced.

6.2. Calculation of the local thermal conductivity

The local thermal conductivity of the fuel at the measurement temperature, $\lambda(T)$, was obtained from:

$$\lambda(T) = \alpha(T)\rho(T)C_p(T), \tag{3}$$

where $\alpha(T)$ is the measured local thermal diffusivity, $\rho(T)$ is the local fuel density and $C_p(T)$ is the heat capacity. The local fuel density, ρ was obtained from the percentage theoretical density, % TD, which is defined as

$$\%\ \mathrm{TD} = \frac{\rho}{\rho_{\mathrm{th}}} \cdot 100, \tag{4}$$

where ρ_{th} is the theoretical density of UO_2, which was taken to be 10.96 g cm^{-3}. The percentage theoretical density was calculated using the following expression:

$$\%\mathrm{TD} = 100 - \left[P + \left\{\frac{B}{10} \times \left(\left(\frac{\Delta V}{V}\right)_{\text{solid FP}} + \left(\frac{\Delta V}{V}\right)_{\text{matrix gas}} \times f^{\mathrm{Xe}}\right)\right\}\right], \tag{5}$$

where % TD is the percentage theoretical density, P is the local porosity, B is the local burn-up in MWd/kgHM, $\left(\frac{\Delta V}{V}\right)_{\text{solid FP}}$ is the matrix swelling rate due to solid fission products (0.32% per 10 MWd/kgHM burn-up), $\left(\frac{\Delta V}{V}\right)_{\text{matrix gas}}$ is the matrix swelling rate due to fission gas in solution (0.56% per 10 MWd/kgHM see e.g., Ref. [29]) and f^{Xe} is the local fraction of retained Xe measured by EPMA. The local burn-up, local porosity and local fraction of retained Xe at some radial positions where the thermal diffusivity was measured are given in Table 4. The fuel density at the measurement temperature, $\rho(T)$, was calculated from the linear thermal expansion of UO_2 using the expression

$$\rho(T) = \rho(273)\left(\frac{L_{273}}{L_{\mathrm{T}}}\right)^3, \tag{6}$$

where $\rho(273)$ is the density of UO_2 at 273 K (10.96 g cm^{-3}) and L and L_{273} are the lengths at the measurement temperature T (in K) and at 273 K, respectively. The increase of a unit length of UO_2 was calculated using the fourth order polynomial for the linear thermal expansion coefficient for UO_2 given by Martin [30] and recommended by Fink [31].

$$L = L_{273}(9.973 \times 10^{-1} + 9.082 \times 10^{-6}T - 2.705 \times 10^{-10}T^2 + 4.391 \times 10^{-12}T^3). \tag{7}$$

The heat capacity of irradiated fuel at the measurement temperature was taken equal to that of unirradiated UO_2. According to Lucuta et al. [8] in the temperature range 25–1500 °C, the heat capacity of stoichiometric irradiated UO_2 at a burn-up of 85 MWd/kgHM is only 1.5% higher than that of the unirradiated material. The heat capacity $C_p(T)$ of unirradiated UO_2 in J mol^{-1} K^{-1} at the temperature of the thermal diffusivity measurement was calculated from the six term polynomial (Eq. (8)) given by Fink [31].

Table 4
Values of the quantities used to calculate the density of the fuel at some radial positions where thermal diffusivity measurements were made

Radial position (r/r_0)	Local burn-up[a] (MWd/kgHM)	Porosity (vol.%)	Xe fractional retention[b]
0.08	88	3.3	0.128
0.36	88	5.8	0.137
0.47	88.7	5.8	0.137
0.55	88.7	5.8	0.135
0.57	89.4	6.7	0.138
0.68	92.2	10.3	0.156
0.79	99.7	10.3	0.142
0.81	99.8	10.3	0.140

[a] From the local concentration of fission product Nd measured by EPMA.
[b] Gas in solution in the fuel matrix as measured by EPMA. The amount of Xe created in the fuel pellet is assumed to correspond to 1.5 wt%.

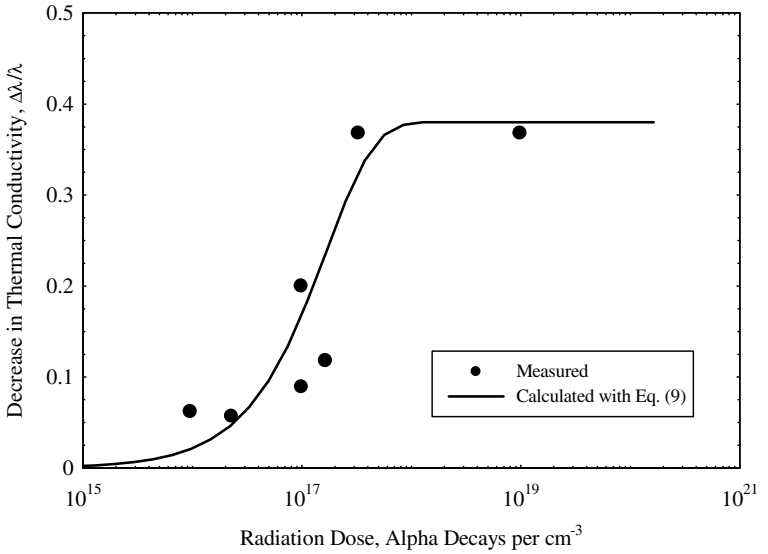

Fig. 8. Relative decrease in the thermal conductivity of UO_2 doped with 0.1 and 10 wt% Pu at 280 °C as a function of accumulated α-radiation dose during storage.

$$C_\rho(T) = +52.1743 + 87.951t - 84.2411t^2 + 31.542t^3 - 2.6334t^4 + 0.71391t^{-2}, \quad (8)$$

where $t = T/1000$ and T is the temperature in K.

Unless otherwise stated the thermal conductivity values reported in the present paper have not been normalised to 5% porosity, which is frequently done to allow comparison of data from different laboratories.

6.3. Elucidation of the influence of self-irradiation during storage on thermal conductivity

The decrease in the thermal conductivity due to radiation damage during storage was obtained from the radiation dose, i.e., from the accumulated alpha decay. This in turn was calculated from the specific activity of the fuel and time elapsed between discharge of the fuel from the reactor and the measurement of the thermal diffusivity. At the radial positions where the thermal diffusivity was measured, the local specific activity was derived from the local Pu concentration measured by EPMA (see Fig. 3), which was assumed to be representative of the local concentration of the actinide isotopes in total.

The influence of alpha radiation dose on the thermal conductivity was determined from thermal diffusivity measurements made at 280 °C on samples of UO_2 doped with 0.1 and 10 wt% ^{238}Pu and stored for different lengths of time. As seen from Fig. 8, in agreement with the findings of Schmidt et al. [32], the percentage change in thermal conductivity with radiation dose can be described by an Arrhenius type equation of the form

$$\Delta\lambda/\lambda = 0.38[1 - \exp(-yn_\alpha)], \quad (9)$$

where y is the rate constant of Schmidt et al. [32] (5.88×10^{-18} cm^3) and n_α is accumulated number of alpha disintegrations per cm^3.

From the isotopic composition of the actinide elements measured by ICP-MS (see Table 3) the specific activity of the fuel was calculated to be 4.5 GBq g^{-1}. More than 95% of this activity was generated by ^{244}Cm. During the time that had elapsed between discharge of the fuel from the reactor and the measurement of the thermal diffusivity (64 months for the sample on which the thermal diffusivity was measured at $r/r_0 = 0.55$ and 88 months in the case of the other sample) the order of magnitude of the accumulated alpha dose was 10^{18} disintegrations per cm^3. Fig. 8 indicates that at this high radiation dose, the relative decrease in the thermal conductivity was very close to its maximum value of 38%.

7. Results

7.1. Influence of annealing temperature on thermal diffusivity

The influence of thermal annealing at temperatures up to 840 °C on the local thermal diffusivity of the high burn-up fuel close to the mid-radial

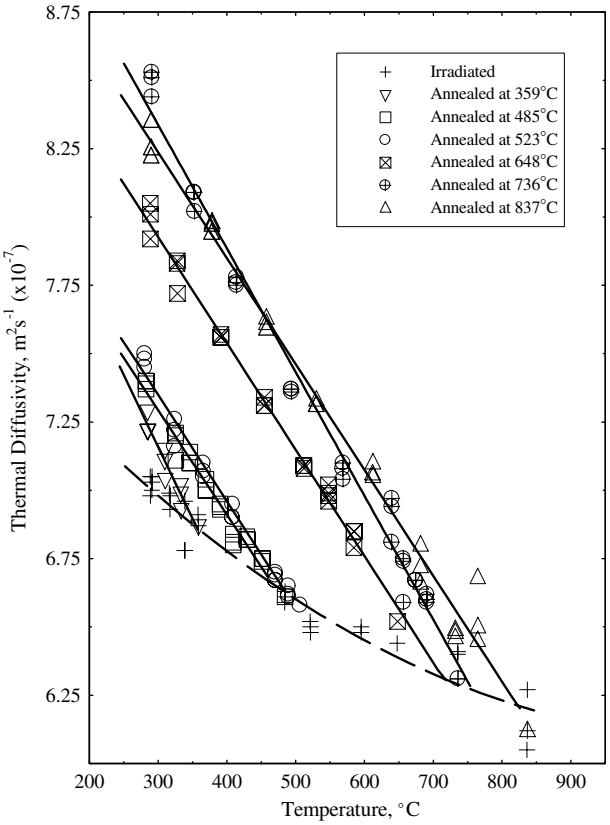

Fig. 9. Thermal diffusivity of the high burn-up fuel at $r/r_0 = 0.55$ before and after annealing. The error on the thermal diffusivity values is of the order of ±5%.

pellet position is shown in Fig. 9. It can be seen that in the irradiated condition the thermal diffusivity decreased from about $7.1 \times 10^{-7}\,m^2\,s^{-1}$ at 250 °C to $6.2 \times 10^{-7}\,m^2\,s^{-1}$ at 840 °C. On cooling from a given temperature in this range the thermal diffusivity increased steeply with decrease in temperature. Table 5 gives the local thermal diffusivity of the fuel at $r/r_0 = 0.55$ as measured at 300 °C after annealing at successively higher temperatures. It can be seen that annealing at 523 °C caused the thermal conductivity of the fuel at 300 °C to increase by around 5%, whereas annealing the fuel at 837 °C increased the thermal diffusivity by about 18%.

Table 5
Thermal diffusivity at 300 °C of the high burn-up fuel at $r/r_0 = 0.55$ in the irradiated condition and after annealing at temperatures in the range 359–837 °C

Run no.	Annealing temperature (°C)	Thermal diffusivity at 300 °C ($m^2\,s^{-1}$) ($\times 10^{-7}$)	$\Delta\alpha/\alpha$ (%)
Irradiated condition[a]		6.98	
1	359	7.16	2.6
2	485	7.29	4.4
3	523	7.35	5.3
4	648	7.93	13.6
5	736	8.34	19.4
6	837	8.24	18.1

[a] Including self-irradiation during storage prior to measurement of the thermal diffusivity.

7.2. Variation in thermal diffusivity with radial position

Fig. 10 shows the radial variation of the thermal diffusivity of the fuel at 217 °C (the lowest temperature at which measurements were made) in the irradiated condition and after annealing to 452 °C in two steps. In all three cases, the thermal diffusivity decreases from the centre to the surface of the fuel pellet. In the radial interval in which thermal diffusivity was measured, $r/r_0 = 0.08$–0.81, the thermal diffusivity of the high burn-up fuel at 217 °C decreased from about $8.0 \times 10^{-7}\,m^2\,s^{-1}$ at $r/r_0 = 0.08$ to

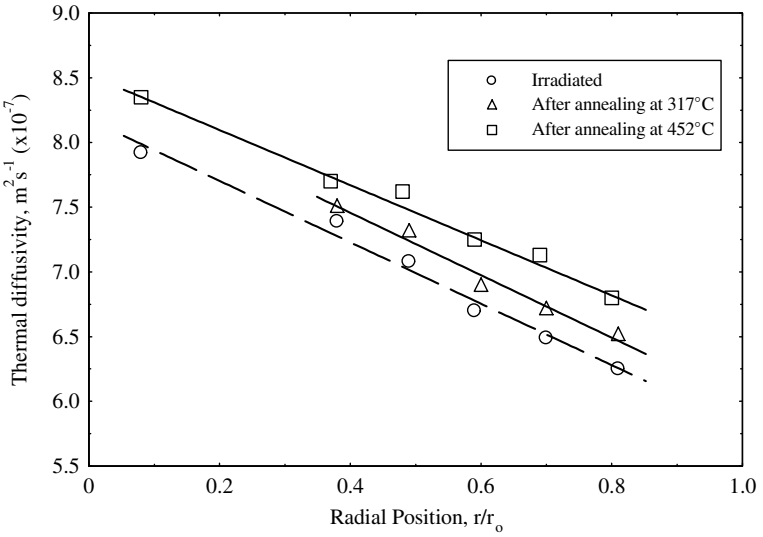

Fig. 10. Radial variation of the thermal diffusivity of the high burn-up fuel at a temperature of 217 °C before and after annealing at 317 and 452 °C. The error on the thermal diffusivity values is of the order of ±5%.

Table 6
Thermal diffusivity of the high burn-up fuel at 217 °C at various radial positions after irradiation and following annealing at 317 and 452 °C

Radial position r/r_0	Thermal diffusivity ($m^2 s^{-1}$) ($\times 10^{-7}$)		
	Irradiated	Annealed 317 °C	Annealed 452 °C
0.1	7.94	–	8.31 (4.7)
0.4	7.23	7.45 (3.0)	7.66 (6.0)
0.8	6.28	6.50 (3.5)	6.82 (8.6)

The percentage change in the thermal diffusivity is given in parentheses.

6.3×10^{-7} m^2 s^{-1} at $r/r_0 = 0.81$, a drop of almost 25%. The effect of annealing on the local thermal diffusivity of the high burn-up fuel at $r/r_0 = 0.1$, 0.4 and 0.8 is summarised in Table 6. It can be seen that after annealing the thermal diffusivity of the fuel was higher. It is also evident that the increase in thermal diffusivity at 217 °C caused by annealing at 452 °C was noticeably higher in the outer region of the fuel than in the central region of the fuel (cf., values at $r/r_0 = 0.8$ and 0.1).

7.3. Influence of annealing temperature on thermal conductivity

The influence of thermal treatment on the local thermal conductivity of the high burn-up fuel close to the mid-radial pellet position is shown in Fig. 11. In appearance, the figure is similar to Fig. 9, which contains the thermal diffusivity results. Like the thermal diffusivity, the thermal conductivity of the irradiated fuel decreases with rise in temperature; in the case of the thermal conductivity from 2.0 W m^{-1} K^{-1} at 300 °C to 1.9 W m^{-1} K^{-1} at 850 °C. Moreover, like the thermal diffusivity, the thermal conductivity increases steeply as the fuel is cooled from the annealing temperature. The increase in the thermal conductivity at 300 °C after annealing the high burn-up fuel at various temperatures in the range 359–837 °C is presented in Fig. 12. It can be seen that following an initial gradual rise in the temperature range 300–500 °C, the thermal conductivity increases sharply reaching a maximum value of approximately 2.4 W m^{-1} K^{-1} at of about 700 °C.

7.4. Variation in thermal conductivity with radial position

Fig. 13 shows the radial variation of the thermal conductivity of the high burn-up fuel at 217 °C in the irradiated condition and following annealing at 452 °C. In the irradiated condition, following a linear decrease in the central region of the fuel, the thermal conductivity exhibits a step in the region between $r/r_0 = 0.55$ and 0.66. As can be seen from Table 7, in the irradiated condition the thermal conductivity of the fuel decreased from 2.20 W m^{-1} K^{-1} at $r/r_0 = 0.2$ to 1.67 W m^{-1} K^{-1} at $r/r_0 = 0.8$. After annealing at 452 °C, the thermal

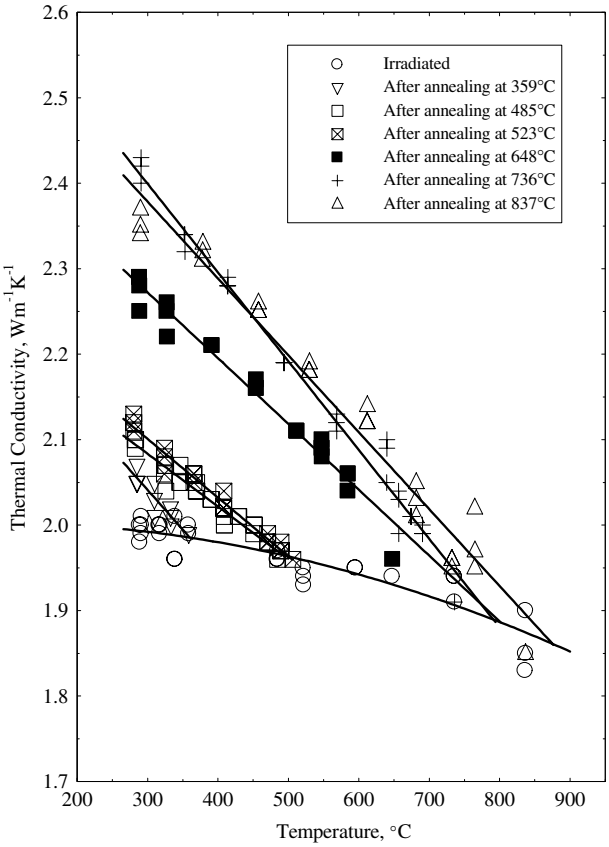

Fig. 11. Thermal conductivity of the high burn-up fuel at $r/r_0 = 0.55$ before and after annealing.

conductivity at 217 °C had risen by 5% at $r/r_0 = 0.2$ and by about 7% at $r/r_0 = 0.8$. Moreover, the step between $r/r_0 = 0.55$ and 0.66 is virtually imperceptible.

It is pointed out that the existence of a step in the conductivity curve for the irradiated condition is confirmed when the thermal conductivity values are plotted against the local fuel temperature (see Fig. 17).

8. Discussion

8.1. Relevance of the HBRP and NFIR fuel disc data

In Fig. 14 Kinoshita's [16] plot of the thermal diffusivity of the NFIR and HBRP fuel discs in the irradiated state as a function burn-up is reproduced with the addition of data points for thermal diffusivity of the high burn-up fuel at $r/r_0 = 0.08$ and 0.81. The fuel disc data represents the thermal diffusivity of UO_2 fuel under specific conditions of irradiation temperature, porosity, microstructure and concentration of fission products in solid solution. Consequently, the data is not directly transferable to power reactor fuel of equivalent burn-up because the quantities referred to above vary with radial position in the fuel pellet. Thus, it is evident from Fig. 14 that, whereas the thermal diffusivity of the high burn-up fuel at $r/r_0 = 0.81$ is in excellent agreement with that of disc fuel of similar burn-up, at $r/r_0 = 0.08$ the thermal diffusivity of the high burn-up fuel is markedly higher. The cause of this inconsistency is the fact that at $r/r_0 = 0.81$ the irradiation temperature, microstructure and porosity of the high burn-up fuel was comparable to that of the disc fuel, whereas at $r/r_0 = 0.08$ they were significantly different. For example, at $r/r_0 = 0.08$ the high burn-up fuel was characterised by thermal restructuring in contrast to the disc fuel which exhibited the high burn-up structure at 88 MWd/kgU.

8.2. Factors determining the thermal conductivity of the high burn-up fuel

In Fig. 15 the variation in the coefficients A and B of Eq. (2) with temperature at $r/r_0 = 0.55$ in the

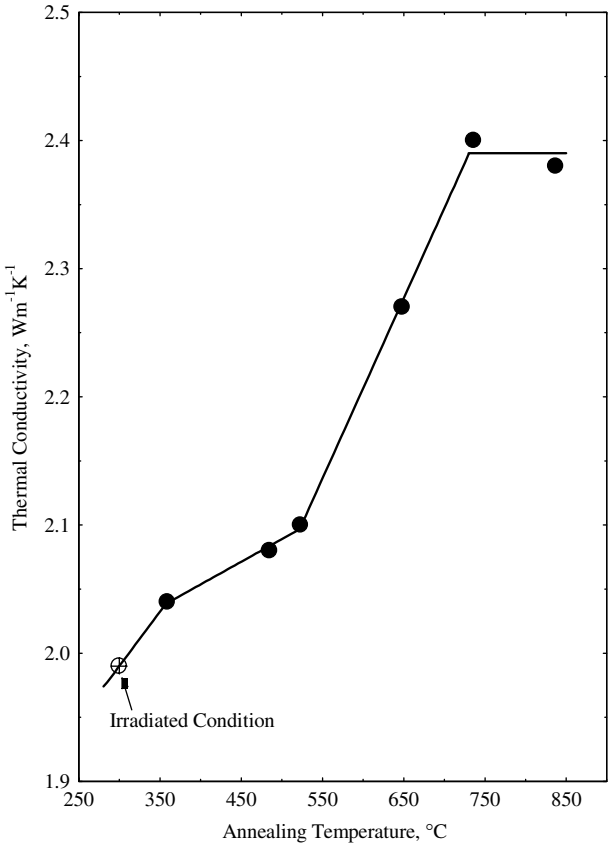

Fig. 12. Thermal conductivity of the high burn-up fuel at 300 °C as a function of annealing temperature in the range 359–837 °C. The line connecting the data points serves to guide the eye.

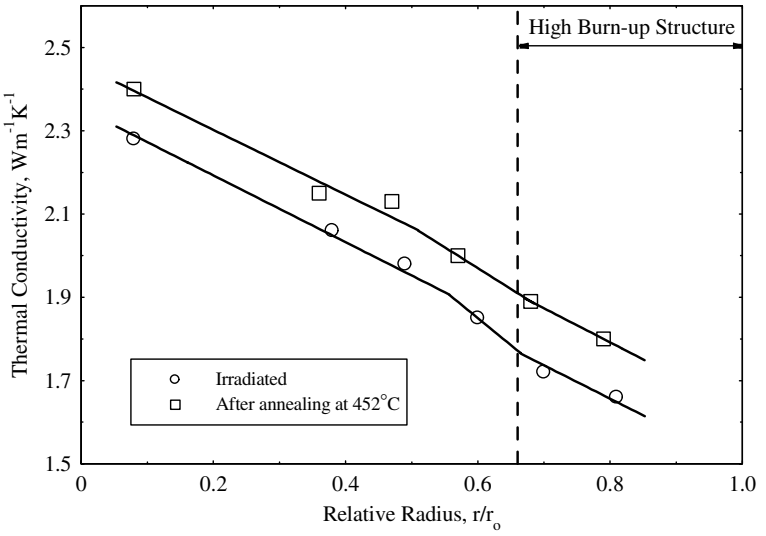

Fig. 13. Radial variation in the thermal conductivity of the high burn-up fuel at 217 °C in the irradiated state and after annealing at 452 °C.

Table 7
Thermal conductivity of the high burn-up fuel at various radial positions at 217 °C in the irradiation condition and after annealing at 452 °C

Radial position (r/r_0)	Thermal conductivity ($W\,m^{-1}\,K^{-1}$)		$\Delta\lambda/\lambda$ (%)
	Irradiated condition	After annealing at 452 °C	
0.2	2.19	2.30	5.0
0.4	2.03	2.15	5.9
0.7	1.72	1.87	8.7
0.8	1.67	1.79	7.2

high burn-up fuel are shown. In addition to experimental data points, values calculated using the mathematical expressions formulated by Ronchi et al. [13] are included for the purposes of comparison. It can be seen that for both coefficients A and B the agreement between the experimental and predicted values is impressive, indicating that the theoretical models proposed by Ronchi et al. [13] accurately describe the mechanisms determining the thermal conductivity of irradiated UO_2 fuel. As is evident from Fig. 15 the models of Ronchi et al. [13] reveal that the recovery of the thermal conductivity of the high burn-up fuel during annealing occurs in two distinct steps. The first step occurs in the temperature range 800–1000 K (527–727 °C) and is characterised by a sharp decrease in the value of A of approximately 0.1 $K\,mW^{-1}$ and a steep increase in the value of B of about $5.0 \times 10^{-5}\,mW^{-1}$. The second step occurs in the temperature range 1150–1400 K (877–1127 °C) and is characterised by drop in the value of A by a similar magnitude to that denoting the first step, and an increase in the value of B of about $8.0 \times 10^{-5}\,mW^{-1}$, which is larger than that associated with the first step. A similar two step process was reported by Ronchi et al. [13] for the recovery of the thermal conductivity of an HBRP disc fuel that was irradiated to a low burn-up of 35 MWd/kgU at a temperature of 480 °C. From the investigation of the influence of self-irradiation on the thermal conductivity of UO_2 doped with 0.1 and 10 wt% ^{238}Pu [33] it is almost certain that the first recovery step is associated with the annihilation of point defects that were created out-of-pile during storage of the spent fuel before the thermal diffusivity measurements were made (64 months). The fact that the first recovery step is complete at a temperature lower than the irradiation temperature at $r/r_0 = 0.55$ during the last reactor cycle is taken as evidence that the healing of in-pile irradiation damage is not involved to any significant degree in this step. The second step is assumed to be associated with the annihilation of in-pile radiation damage and the removal of fission product atoms from the fuel lattice, particularly Xe and Cs atoms, which coalesce to form nano-bubbles and nano-precipitates. As will have already been noted, the experimental data

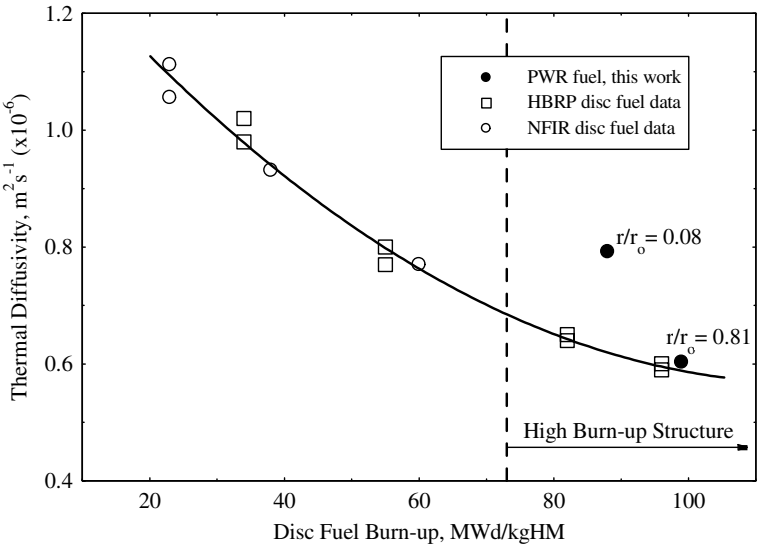

Fig. 14. Variation in the thermal diffusivity of irradiated UO_2 fuel with burn-up at 300 °C, Irradiation temperature: HBRP disc fuel 405–460 °C; NFIR disc fuel 600 °C (end-of-life). High burn-up fuel this work, at $r/r_0 = 0.08$ 930 °C, at $r/r_0 = 0.81$, 600 °C (last irradiation cycle).

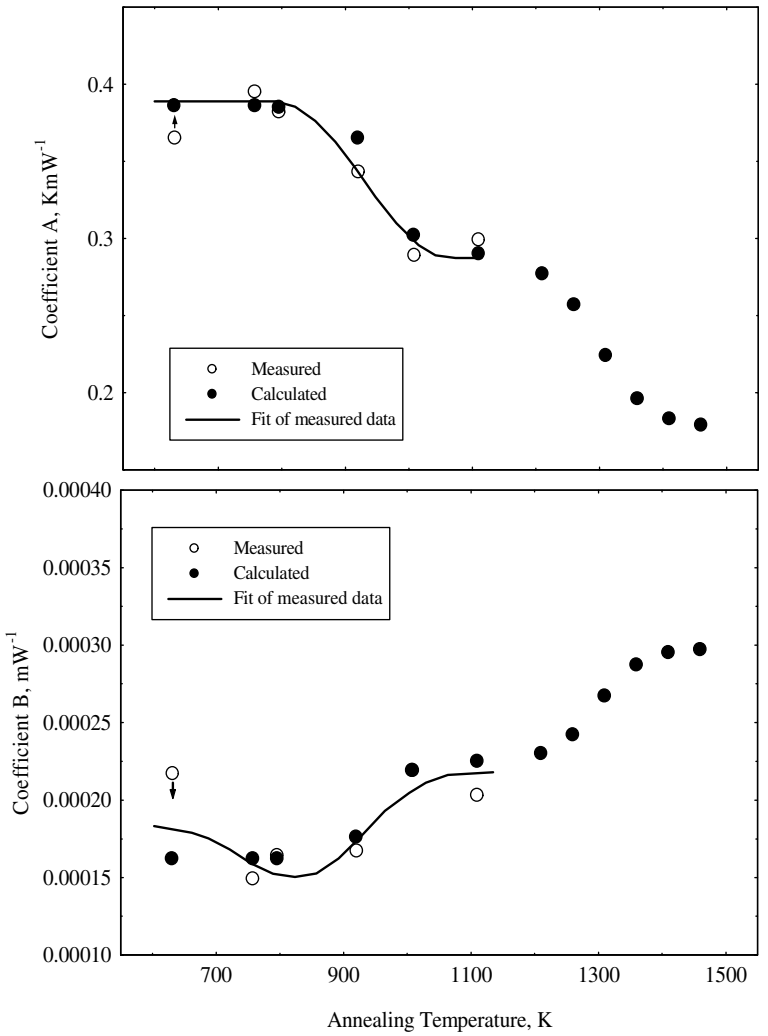

Fig. 15. Variations in the coefficients A and B in the thermal conductivity formula $\lambda = 1/(A + BT)$ for the high burn-up fuel.

points in Fig. 15 are restricted to annealing temperatures up to 1110 K (837 °C) and cover the first recovery step only. At this temperature, the sample began to fragment, and the thermal diffusivity measurements were abandoned. Experience has shown that at high burn-up the fuel disc samples on which thermal diffusivity measurements are carried out break when the annealing temperature exceeds the irradiation temperature by only a few degrees. Thus, the temperature threshold for fragmentation can be used as an indicator of the reliability of the calculated radial temperature profile during the last reactor cycle. The temperature at $r/r_0 = 0.55$ during the last irradiation cycle was calculated to be 800 °C (see Fig. 1), which is 40 °C below which the measurements were halted because the sample had begun to break. This reveals that the temperature history for the high burn-up rod calculated with the computer code CARO-E [24] is accurate to a high degree. It is also evident from Fig. 15 that the experimental points for the values of the coefficients A and B at the lowest annealing temperature of 632 K (359 °C) are incorrect. The error is due to the large uncertainties on the intercept and slope of the regression line, which arise because the thermal diffusivity measurements were made in a narrow temperature range of 75 °C.

8.3. Recovery of thermal conductivity due to the healing of out-of-pile radiation damage

As reported in Section 6.3. the alpha-radiation dose accumulated by the high burn-up fuel during the storage was of the order of 10^{18} disintergrations

per cm^3. As seen from Fig. 8, this radiation dose should result in a significant decrease in the thermal conductivity of the high burn-up fuel during storage. Nevertheless, the recovery in the thermal conductivity measured at 217 °C after annealing at 452 °C amounted to 5–9% of the irradiated value (Table 7). Thus, a temperature of 452 °C was clearly insufficient to remove the bulk of the point defects created by alpha decay during storage of the spent fuel. This is consistent with the finding that the coefficient A in Eq. (2) varies little with annealing temperature below 800 K (527 °C). The latter being the onset temperature for the first recovery step associated with the removal of out-of-pile radiation damage (see Fig. 15).

8.4. Effect of the high burn-up structure on the thermal conductivity of UO_2 fuel

It is evident from Fig. 14 that the formation of the high burn-up structure produced a marked increase in the thermal diffusivity and hence in the thermal conductivity in the outer region of high burn-up fuel. The data points in Fig. 14, with the exception of that for $r/r_0 = 0.08$ in the high burn-up fuel, are reproduced in Fig. 16 and regression lines are drawn through the data points at burn-ups below 60 MWd/kgHM, which is generally taken as the local burn-up threshold for the formation of the high burn-up structure, and through the data points above 80 MWd/kgHM at which a large percentage of the fuel microstructure has been transformed to the high burn-up structure. If it is accepted that the regression line for the data below 60 MWd/kgHM represents the changes in the thermal diffusivity of the fuel due to the build-up of fission products and in-pile irradiation damage with burn-up, then it is apparent that if the high burn-up structure had not formed the thermal diffusivity at 100 MWd/kgHM, would have fallen to $3.8 \times 10^{-7}\ m^2\ s^{-1}$. As a consequence of the formation of the high burn-up structure, however, the thermal diffusivity of the fuel at 100 MWd/kgHM is actually $5.9 \times 10^{-7}\ m^2\ s^{-1}$; that is, 55% higher than the value expected to result from the degradation caused by the build-up of fission products and point defects in the fuel lattice at this burn-up. Clearly, the increase in thermal diffusivity and conductivity caused by the formation of the high burn-up structure is a consequence of the removal of fission product atoms from the fuel lattice and healing of radiation defects that accompanies recrystallisation of the fuel grains (part of the formation process of the high burn-up structure). Evidently, the decrease in thermal diffusivity and conductivity caused by the porosity of the high burn-up structure is small compared with the increase caused by the fall in the concentrations of impurity atoms and point defects in the lattice.

The role of the pores of the high burn-up structure as sinks for the fission gas expelled from the

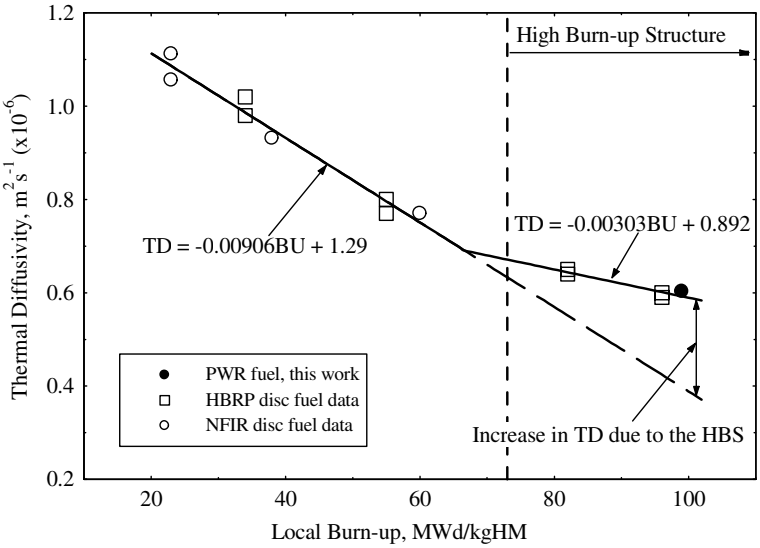

Fig. 16. Influence of the presence of the high burn-up structure on the thermal diffusivity of the high burn-up fuel. In the outer region of the fuel at a local burn-up of 100 MWd/kgHM the high burn-up structure increases the thermal diffusivity by 50%. The vertical broken line marks the burn-up at which the HBRP disc fuel had fully transfórmed to the high burn-up structure.

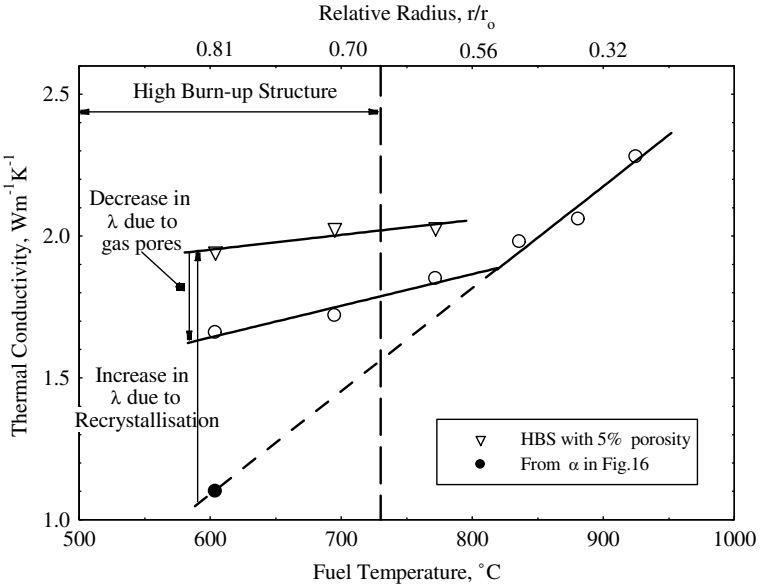

Fig. 17. Thermal conductivity of the high burn-up fuel at 217 °C as a function of the local radial temperature during the last irradiation cycle. The high burn-up structure markedly increases the local thermal conductivity of the fuel in the region in which forms. Five percent of porosity is a hypothetical value equating with the porosity of the fuel prior to irradiation. The thermal conductivity of recrystallised fuel with 5% porosity was calculated using the equation of Brandt and Neuer [34], Eq. (10) in this paper.

fuel lattice during recrystallisation is more important than their effect as barriers to heat transport. In Fig. 17 the local thermal conductivity of the high burn-up fuel is plotted against the local radial temperature during the last irradiation cycle. Regression lines are drawn through the data points lying between the fuel centre and $r/r_0 = 0.5$ and through the data points in the outer region of the fuel at $r/r_0 = 0.6$, 0.7 and 0.81. The former line represents the effect of temperature on the thermal conductivity of the fuel at a burn-up of about 90 MWd/kgHM and a porosity of 3–6%. It reveals that if the high burn-up structure had not formed the thermal conductivity of the fuel would have fallen to at least 1.1 W m^{-1} K^{-1} at $r/r_0 = 0.81$. (The same conductivity value is calculated from the thermal diffusivity data in Fig. 16 if the as-fabricated fuel density of 95% TD is taken for the untransformed fuel.) Also shown in Fig. 17 is the thermal conductivity of the recrystallised fuel in the outer region of the pellet assuming it to contain 5% porosity instead of the higher measured values of 8 and 10.3% (see Fig. 5). It can be seen that the thermal conductivity of the less porous, recrystallised fuel is substantially higher than that calculated from the measured local thermal diffusivity and the measured local porosity. The thermal conductivity of the recrystallised fuel at 5% porosity was calculated using Eq. (10), which is recommended by Brandt and Neuer [34] for this purpose.

$$\lambda_0 = \frac{\lambda_p}{[1 - \alpha P]}, \quad \alpha = 2.6 - 05t, \tag{10}$$

where P is the porosity fraction, λ_p is the thermal conductivity of UO_2 with porosity P, λ_0 is the thermal conductivity of UO_2 of theoretical density, and $t = T(°C)/1000$.

From Fig. 17 it is clear that recrystallisation increased the thermal conductivity in the outer region of the fuel at 217 °C by between 29% and 77%, whereas the porosity created by the gas swept out of the grains resulted in a decrease of 11–15%. It will be noted that the inflection in the radial thermal conductivity profile does not occur at $r/r_0 = 0.66$, which is the penetration limit of the high burn-up structure reported by Manzel and Walker [23], but deeper in the fuel at $r/r_0 = 0.51$. Between $r/r_0 = 0.51$ and 0.66, however, the fuel microstructure is closely related to the high burn-up structure (see Fig. 9, Ref. [23]). It is a mixture of untransformed and recrystallised UO_2 grains. The porosity in this region also increases (see Fig. 5) as the extent of recystallisation increases. The pores, however, do not exhibit the facetted morphology that is characteristic of the gas

pores of the high burn-up structure. This can be accounted for by the fact that at the radial positions in question recrystallisation had been preceded by thermal fission gas release earlier in the irradiation [23]. The increase in thermal conductivity found between $r/r_0 = 0.51$ and 0.66 is undoubtedly a consequence of the occurrence of recrystallisation in this region.

As already mentioned the fuel disc samples used for laser flash measurements exhibit a propensity to fragment during recovery studies when the annealing temperature exceeds the local irradiation temperature in the last reactor cycle. Regrettably, the disc sample used to investigate the variation in the thermal diffusivity with radial position fragmented at about 610 °C. This corresponds to the irradiation temperature at $r/r_0 = 0.81$ (see Fig. 1), which means that the thermal diffusivity measurements on the sample were all made at temperatures below the irradiation temperature in the last fuel cycle. In fact, depending on the radial position the difference between the maximum annealing temperature of 452 °C and the irradiation temperature in the last cycle varied from 153 °C at $r/r_0 = 0.81$ to 385 °C at $r/r_0 = 0.08$. Consequently, the recovery in the thermal conductivity observed during annealing was that resulting from the healing of self-radiation damage during the storage of the fuel.

9. Conclusions

The thermal conductivity of UO_2 nuclear fuel decreases with burn-up. The decrease is mainly caused by the build-up of fission product atoms and point defects resulting from radiation damage in the UO_2 lattice, both of which act as scattering centres for phonons. Thermal annealing of the spent fuel results in the recovery of the thermal conductivity. This occurs in two distinct steps. The first step occurs in the temperature range 800–1000 K (527–727 °C) and is associated with the removal of point defects produced by out-of-pile radiation damage. The second step occurs in the temperature range 1150–1400 K (877–1127 °C) and is attributed to further annealing of self-irradiation, the onset of annihilation of in-pile radiation damage and the removal of fission product atoms in solid solution in the fuel matrix to form voids and precipitates. Thermal annealing at temperatures below 800 K (527 °C) results in slight recovery of the thermal conductivity amounting to less than 10% of the value for the irradiated fuel. This recovery is due to the partial healing of point defects created by self-irradiation in the time interval between discharge of the spent fuel from the reactor and the measurement of the thermal diffusivity. The bulk of the damage created during this time is removed in the first recovery step. The formation of the high burn-up structure has a very positive effect on the thermal conductivity in the outer region of the fuel. The thermal conductivity in this region of the fuel is much higher than would be the case if the high burn-up structure was not present. The increase in thermal conductivity caused by the formation of the high burn-up structure is a consequence of the removal of fission product atoms and radiation defects from the fuel lattice during recrystallisation of the fuel grains (an integral part of the formation process of the high burn-up structure). The role of the pores of the high burn-up structure as sinks for fission gas expelled from the fuel lattice during recrystallisation is more important than their effect as barriers to heat transfer. In the outer region of the fuel, between $r/r_0 = 0.81$ and 0.66, the porosity of the high burn-up structure reduced the increase in thermal conductivity caused by recrystallisation by between 35 and 50% at 217 °C.

Acknowledgements

The work presented in this paper is part of a long-standing high burn-up programme being performed by AREVA-Framatome ANP and the Swiss nuclear plant Goesgen. The authors would like to thank Goesgen for their fruitful co-operation and their continuing support.

References

[1] C.T. Walker, T. Kameyama, S. Kitijma, M. Kinoshita, J. Nucl. Mater. 188 (1992) 73.
[2] J. Spino, K. Vennix, M. Coquerelle, J. Nucl. Mater. 231 (1996) 179.
[3] I.L.F. Ray, Hj. Matzke, H.A. Thiele, M. Kinoshita, J. Nucl. Mater. 245 (1997) 115.
[4] E. Kolstad, C. Vitanza, J. Nucl. Mater. 188 (1992) 104.
[5] W. Wiesenack, in: Proc. ANS Inter. Topical Mtg. on LWR Fuel Performance, ANS La Grange Park, IL, 1997, p. 507.
[6] R.C. Daniel, I. Cohen, Bettis Atomic Power, USA, Report WAPD-246, 1964.
[7] R.O. Lokken, E.L. Courtright, Battelle Pacific Northwest Laboratories, USA, Report BNWL-2270, 1976.
[8] P.G. Lucata, Hj. Matzke, R.A. Verrall, H.A. Tasman, J. Nucl. Mater. 188 (1992) 198.
[9] P.G. Lucuta, R.A. Verrall, H. Matzke, B.J. Palmer, J. Nucl. Mater. 178 (1991) 48.
[10] D. Shaw, L.A. Goldsmith, J. Sci. Instrum. 43 (1966) 594.

[11] H.E. Schmidt, M. van den Berg, L. van der Hoek, High Temp.-High Press. 1 (1969) 309.
[12] P.G. Lucuta, Hj. Matzke, R.A. Verrall, J. Nucl. Mater. 223 (1995) 51.
[13] C. Ronchi, M. Sheindlin, D. Staicu, M. Kinoshita, J. Nucl Mater. 327 (2004) 58.
[14] M. Kinoshita, S. Kitajima, T. Kameyama, T. Matsumura, E. Kolstad, Hj. Matzke, in: Proc. ANS Topical Mtg. on LWR Fuel Performance, Portland, OR, USA (ANS La Grange Park, IL), 1997, p. 530.
[15] S.K. Yagnik, in: Proc. ANS Topical Mtg. on LWR Fuel Performance, Park City, UT, USA (ANS La Grange Park, IL), 2000, p. 634.
[16] M. Kinoshita, T. Sonoda, S. Kitajima, A. Sasahara, E. Kolstad, Hj. Matzke, V.V. Rondinella, A.D. Stalios, C.T. Walker, I.L.F. Ray, M. Sheindlin, D. Halton, C. Ronchi, in: Proc. ANS Topical Mtg. on LWR Fuel Performance, Park City, UT, USA (ANS La Grange Park, IL), 2000, p. 590.
[17] K. Lassmann, C.T. Walker, J. van de Laar, F. Lindström, J. Nucl. Mater. 226 (1995) 1.
[18] M. Mogensen, J.H. Pearce, C.T. Walker, J. Nucl. Mater. 264 (1999) 99.
[19] J.C. Carrol, R.A. Gomme, N.A. Leech, Enlarge Halden Programme Group Meeting, Bolkesjø Norway, 1994, Paper F2.3.
[20] J. Nakamura, T. Kodaira, M. Uchida, T. Yamahara, H. Uetsuka, A. Kikuchi, in: Proc. ANS Topical Mtg. on LWR Fuel Performance, Portland, OR, USA (ANS La Grange Park, IL), 1997, p. 499.
[21] K. Ohira, N. Itagaki, in: Proc. ANS Topical Mtg. on LWR Fuel Performance, Portland, OR, USA (ANS La Grange Park, IL), 1997, p. 541.
[22] I.C. Hobson, R. Taylor, J.B. Ainscough, J. Phys. D: Appl. Phys. 7 (1974) 1003.
[23] R. Manzel, C.T. Walker, J. Nucl. Mater. 301 (2002) 170.
[24] F. Sontheimer, H. Landkron, IAEA Tech. Committee Mtg. on Nuclear Fuel Behaviour at High Burn-up and its Experimental Support. Windermere, UK, June 2000, IAEA-TECDOC-1233, 2001, p. 105.
[25] K. Lassmann, C. O'Carrell, J. van de Laar, C.T. Walker, J. Nucl. Mater. 208 (1994) 223.
[26] C.T. Walker, V.V. Rondinella, D. Papaioannou, S. Van Winkel, W. Goll, R. Manzel, J. Nucl. Mater. 345 (2005) 192.
[27] J. Spino, D. Papaioannou, J. Nucl. Mater. 281 (2000) 146.
[28] M. Sheindlin, D. Halton, M. Musella, C. Ronchi, Rev. Sci. Instrum. 69 (1998) 1426.
[29] J. Spino, J. Rest, W. Goll, C.T. Walker, J. Nucl. Mater. 346 (2005) 131.
[30] D.G. Martin, J. Nucl. Mater. 152 (1988) 94.
[31] J.K. Fink, J. Nucl. Mater. 279 (2000) 1.
[32] H.E. Schmidt, J. Richter, Hj. Matzke, J. Van Geel, in: T. Tong (Ed.), Proc. Thermal Conductivity, vol. 22, Technomic Publishing. Co. Inc., USA, 1994, p. 920.
[33] D. Staicu, T. Wiss, C. Ronchi, in: Proc. ANS Topical Mtg. on LWR Fuel Performance, Orlando, FL, USA (ANS La Grange Park, IL), 2004, Paper 1087.
[34] R. Brandt, J. Neuer, Non-Equilib. Thermodyn. 1 (1976) 3.